THERMODYNAMIC PROPERTIES CALCULATION USING A MULTIOBJECTIVE APPROACH IN ESTIMATING THE PARAMETERS OF THE GEOS3C EQUATION OF STATE

G. R. Silva[a],

T. M. Galo[a],

A. M. Soares Jr.[b],

and L. N. H. G. Oliveira[a]

[a]Universidade do Estado do Rio de Janeiro
Instituto Politécnico
Nova Friburgo, Rio de Janeiro, Brasil
grsilva@iprj.uerj.br
taniamaria@iprj.uerj.br
nelio@iprj.uerj.br

[b]Universidade Estadual Norte Fluminense
Darcy Ribeiro
Laboratório de Engenharia e Exploração de Petróleo
Macaé, Rio de Janeiro, Brasil

Received: Set 20, 2022
Revised: Oct 05, 2022
Accepted: Oct 07, 2022

ABSTRACT

Since van der Waals' first publication, a lot of equations of state have been proposed to represent the PVT behavior of pure compounds, as is the case with GEOS3C, which is a new form of generalized cubic equation of state that uses a temperature function dependent on three adjustable empirical parameters. In order to obtain the parameters that lead to the lowest errors of vapor pressure and saturated liquid volume predictions, it is possible to turn this problem into a multiobjective optimization problem. In this context, a modified MOPSO algorithm was employed. This method has the main advantage to provide a set of solutions that show the existing conflict in the attempt to minimize the properties of interest. Substances from different chemical families were used to evaluate the methodology proposed in this work and comparisons against experimental data were made. Results showed that the values obtained through multiobjective optimization for GEOS3C adjustable parameters provide better or equivalent predictions for all calculated thermodynamic properties. In addition, it was possible to observe a correlation between the parameters in the viable regions of the Pareto fronts: C_1 assuming a constant value, whereas C_2 and C_3 are linearly dependent on each other.

Keywords: equations of state; parameters estimate; multiobjective optimization; thermodynamic properties

NOMENCLATURE

a	specific parameter of the GEOS3C equation of state
a_c	specific parameter of the GEOS3C equation of state
b	specific parameter of the GEOS3C equation of state
B	specific parameter of the GEOS3C equation of state
c	specific parameter of the GEOS3C equation of state
C_1	adjustable parameter of the GEOS3C equation of state
C_2	adjustable parameter of the GEOS3C equation of state
C_3	adjustable parameter of the GEOS3C equation of state
C_p^l	heat capacity at constant pressure of the liquid phase
C_p^v	heat capacity at constant pressure of the vapor phase
C_v^l	heat capacity at constant volume of the liquid phase
C_v^v	heat capacity at constant volume of the vapor phase
d	specific parameter of the GEOS3C equation of state
$\vec{f}$	vector of objective functions
g_i	inequality constraints functions
h_i	equality constraints functions
N_p	number of experimental data points
P	pressure
P_c	critical pressure
P_r	reduced pressure
P_s	saturation (or vapor) pressure
R	universal gas constant
R_1	constant of Rackett's correlation
R_2	constant of Rackett's correlation
R_3	constant of Rackett's correlation
R_4	constant of Rackett's correlation
T	temperature
T_c	critical temperature
T_r	reduced temperature
V	molar volume
V_l	saturated liquid volume
V_r	reduced volume
V_v	saturated vapor volume
W_1	constant of Wagner's correlation
W_2	constant of Wagner's correlation
W_3	constant of Wagner's correlation

W_4 constant of Wagner's correlation
W_5 constant of Wagner's correlation
$\vec{x}$ vector of decision variables
$\vec{x}^*$ vector of optimal solutions
Z_l root corresponding to the liquid phase

Greek symbols

α_c Riedel's criterion
β temperature correction function
ΔC_p^{vap} heat capacity at constant pressure of vaporization
ΔC_v^{vap} heat capacity at constant volume of vaporization
ΔH^{vap} enthalpy of vaporization
ΔS^{vap} entropy of vaporization
ΔU^{vap} internal energy of vaporization
ω acentric factor
Ω_a specific parameter of the GEOS3C equation of state
Ω_b specific parameter of the GEOS3C equation of state
Ω_c specific parameter of the GEOS3C equation of state
Ω_d specific parameter of the GEOS3C equation of state

Subscripts

exp experimental
eos equation of state

INTRODUCTION

For many engineering applications, thermodynamic properties can be estimated accurately in situations where there is no reliable experimental data. Although there are several empirical and generalized correlations for the calculation of saturated liquid volumes, the estimation of saturation properties through equations of state has numerous advantages, especially in the simulation of phase equilibrium problems. Process engineers, for example, use equations of state as a tool to predict phase equilibrium problems and thermophysical properties of fluids in order to design equipments and processes (Abdollahi-Demneh *et al.*, 2010).

Since the emergence of van der Waals model, a lot of equations of state have been proposed to represent thermodynamic properties of pure compounds and mixtures. In most of the situations, the use of cubic equations of state satisfactorily keeps the commitment between accuracy and computational cost (Patel and Teja, 1982). In this context, Geanã and Feroiu (2000b) proposed a generalized form for the cubic equations of state, called by them GEOS3C, which uses a temperature function dependent on three adjustable parameters (C_1, C_2 and C_3). In their work, the authors obtained these parameters by matching three points on the saturation curve (vapor pressures together with the corresponding liquid volumes), at three fixed temperatures. This practice is very common in the area.

Recently, in the works of Menegazzo *et al.* (2019) and Mota (2019), authors proposed to estimate the parameters of the equations of state studied by them through multiobjective optimization, adjusting the results of the equations of state to two independent data set measurements (saturation pressure and saturated liquid volume of the pure components). The first mentioned authors studied an associated equation of state (composed by a physical part, based on the Peng-Robinson equation of state, and an associating part, calculated through a linear association approach), and the second one, the Patel-Teja equation of state.

Following this methodology, in this work, the adjustable parameters of GEOS3C temperature function are estimated through multiobjective optimization in order to obtain lower errors for vapor pressures and saturated liquid volumes predictions. A modified MOPSO algorithm, that uses the ε-dominance criteria to avoid problems of purely numerical dominance, a simplified storage management system to promote a better particles distribution and a fixed global leadership for a certain number of iterations, was employed in this process. Substances from different chemical families were used to evaluate the methodology proposed in this work, comparing the obtained results with experimental data available in the literature.

GEOS3C EQUATION OF STATE

The general cubic equation of state (GEOS) has the following form

$$P = \frac{RT}{V-b} - \frac{a(T)}{(V-d)^2 + c} \tag{1}$$

where P is pressure, R is universal gas constant, T is temperature and V is volume.

The parameters a, b, c and d, presented in Eq. (1), for a pure component are expressed by

$$a = a_c \beta^2 (T_r) \tag{2}$$

$$b = \Omega_b \frac{RT_c}{P_c} \tag{3}$$

$$c = \Omega_c \frac{R^2 T_c^2}{P_c^2} \tag{4}$$

$$d = \Omega_d \frac{RT_c}{P_c} \tag{5}$$

with

$$a_c = \Omega_a \frac{R^2 T_c^2}{P_c} \tag{6}$$

The subscripts r and c in the above equations represent, respectively, the reduced and critical properties of a certain substance.

The new temperature function $\beta(T_r)$, proposed by Geanã and Feroiu (2000b), has the following form

$$\beta(T_r) = \begin{cases} 1 + C_1 y + C_2 y^2 + C_3 y^3, T_r \le 1 \\ 1 + C_1 y, T_r > 1 \end{cases} \tag{7}$$

with

$$y = 1 - \sqrt{T_r} \tag{8}$$

In Geanã and Feroiu (2000b)'s work, temperature function's parameters (C_1, C_2 and C_3) were estimated by matching three points on the saturation curve (vapor pressures together with the corresponding liquid volumes), at three fixed temperatures: triple point, boiling point and reduced temperature $T_r = 0.7$. However, as it will be shown, it is possible to turn this problem into a multiobjective optimization problem.

The expressions of the parameters Ω_a, Ω_b, Ω_c and Ω_d are obtained through the establishment of the following critical conditions (Geanã, 1986) at $T_r = V_r = 1$

$$P_r = 1 \tag{9}$$

$$\left(\frac{\partial P_r}{\partial V_r}\right)_{T_r} = 0 \tag{10}$$

$$\left(\frac{\partial^2 P_r}{\partial V_r^2}\right)_{T_r} = 0 \tag{11}$$

$$\left(\frac{\partial P_r}{\partial T_r}\right)_{V_r} = \alpha_c \tag{12}$$

which lead to the following expressions

$$\Omega_a = (1 - B)^3 \tag{13}$$

$$\Omega_b = Z_c - B \tag{14}$$

$$\Omega_c = (1 - B)^2 (B - 0.25) \tag{15}$$

$$\Omega_d = Z_c - \frac{(1 - B)}{2} \tag{16}$$

where Z_c is the critical compressibility factor of a substance and

$$B = \frac{1 + C_1}{\alpha_c + C_1} \tag{17}$$

Finally, using experimental values for the acentric factor (ω) and for the critical constants, α_c can be expressed by

$$\alpha_c = 5.808 + 4.93\omega \tag{18}$$

MULTIOBJECTIVE PARTICLE SWARM OPTIMIZATION

A multiobjective optimization problem (MOP) can be defined as a problem that involves the simultaneous optimization of two or more objective functions (Coello et al., 2004), ie, to find the vector $\vec{x}^* = [x_1^*, x_2^*, \ldots, x_n^*]^T$ which will satisfy, respectively, the m inequality and the p equality constraints

$$g_i(\vec{x}) \ge 0, i = 1,2,\ldots,m \tag{19}$$

$$h_i(\vec{x}) = 0, i = 1,2,\ldots,p \tag{20}$$

and will optimize the vector function $\vec{f}(\vec{x}) = [f_1(\vec{x}), f_2(\vec{x}), \ldots, f_k(\vec{x})]^T$, where $\vec{x} = [x_1, x_2, \ldots, x_n]^T$ is the vector of decision variables.

In a typical MOP, the objectives are usually conflicting and can be handled by combining them properly to generate the so-called Pareto optimal solutions. Coello and Lechuga (2002) introduced a new approach in which Pareto dominance is incorporated to Particle Swarm Optimization algorithm, so that this heuristic could be able to deal with problems with more than one objective function.

MOPSO version used in this work, named MOPSO Light (MOPSOL), maintains the structure of original PSO (Eberhart and Kennedy, 1995), introducing the following simplified modifications to the algorithm (Soares et al., 2020):

- **Optimality criterion:** ε-dominance criterion, initially implemented by Laumanns et al. (2002), was adopted instead of Pareto dominance, aiming to avoid problems of purely numerical dominance;
- **Storage of global leadership:** the set of leaders particles, that is, the set of nondominated particles, is stored in a fixed size vector, similar to the external repository of Coello and Lechuga (2002), with the objective of promoting a better distribution of the particles in the image;
- **Choice of global leader:** update of leader for each particle of the swarm is done without using any

selection criteria. Global leaders are assigned to the swarm particles sequentially from a randomly chosen first element. In addition, to avoid an erratic movement of the swarm and to accelerate the convergence of particles towards the Pareto front, global leaders are kept fixed for a certain number of iterations, which varies between 3 and 8.

Objective Functions

In this work, the objective functions used to obtain values for GEOS3C equation of state parameters that minimizes the errors for vapor pressure and saturated liquid volume predictions are, respectively:

$$f_1(C_1,C_2,C_3)=\sum_{i=1}^{N_p}\frac{P_{s,i}^{exp}-P_{s,i}^{eos}}{P_{s,i}^{exp}} \quad (21)$$

$$f_2(C_1,C_2,C_3)=\sum_{i=1}^{N_p}\frac{V_{l,i}^{exp}-V_{l,i}^{eos}}{V_{l,i}^{exp}} \quad (22)$$

where values for $P_{s,i}^{exp}$ are calculated using Wagner's correlation (Wagner, 1977)

$$\ln\left(P_{s,i}^{exp}\right)=W_1+\frac{W_2}{T}+W_3\ln(T)+W_4T^{W_5} \quad (23)$$

and values for $V_{l,i}^{exp}$ are calculated using Rackett's correlation (Rackett, 1970)

$$V_{l,i}^{exp}=\frac{R_2^{\left[1+\left(1-T/R_3\right)^{R_4}\right]}}{R_1} \quad (24)$$

In the above expressions, N_p is the number of experimental points.

On the other hand, $P_{s,i}^{eos}$ are calculated based on the algorithm presented by Terron (2009), whereas values for $V_{l,i}^{eos}$ are calculated through the expression $V_{l,i}^{eos}=\frac{Z_lRT}{P_{s,i}^{eos}}$, with Z_l obtained using Cardano's method and Monroy-Loperena's refinement (Monroy-Loperena, 2012).

RESULTS AND DISCUSSION

The main parameters adopted in MOPSO Light simulations are displayed in Table 1. It is important to mention that it was not the subject of this study to analyse the influence of these parameters on the obtained results. The adopted values are more than sufficient for the method to converge.

To evaluate the results obtained through multiobjective optimization, eight substances from different chemical families were chosen, as it can be seen in Table 2. Critical properties and values for the constants required by Wagner and Rackett's correlations (W_i and R_i, respectively) were obtained from the Handbook of Green and Perry (2019).

Table 1. Parameters adopted in MOPSO Light simulations.

Parameter	Value
Total number of particles	1000
Repository size	200
Local learning factor	2.05
Global learning factor	2.05
Minimum inertia weight	0.4
Maximum inertia weight	0.9
Non-linear modulation index	1.2
Number of iterations	300
ε value for ε-dominance criterion	1.0e-05
Number of iterations with a fixed leader	3
Objective space domain	[-5, 5]

Initially, an analysis of the minimum number of experimental points required to obtain stable Pareto fronts is made. In Fig. 1, Pareto fronts obtained for Acetone considering different number of experimental points, $3 \le N_p \le 30$, are presented. In Pareto fronts, the Mean Absolute Percentage Error (MAPE) of vapor pressure and saturated liquid volume are plotted against each other. As it can be observed, in the zoom of Pareto fronts, curves tend to overlap each other for $N_p \ge 7$, ie, up this value there is no significant variation in the obtained results. Therefore, N_p = 10 experimental points leads to stable Pareto fronts and this value was adopted in the following simulations. Similar results were obtained for the other substances.

In Fig. 2, Pareto fronts for the two tested paraffins are shown, as well as a zoom in the viable regions, where chosen parameters give meaningful physical results, keeping both errors under acceptable values. Similar results were obtained for the other substances. In all tested cases, the viable regions were selected using as a cut-off criterion the set of values of the errors associated to the vapor pressure and saturated liquid volume predictions corresponding to the Geanã and Feroiu (2000a)'s parameters. It is worth mention that in the figures of the viable regions, three points are highlighted: lowest vapor pressure error (LVPE), lowest saturated liquid volume error (LSLVE) and intermediate (ITM), the latter being determined by the greatest Euclidean distance from the line connecting the first two.

As it can be observed, ethane's Pareto front is more sharp than methane's and, therefore, one of the objectives (pressure, in this case) varies more than the other over the curve. As an example, to obtain an improvement of 0.01% in the saturated liquid volume prediction, it is necessary to give up 0.26% in the

saturation pressure. In methane's case, on the other hand, the relative change rates from one objective function to the other are balanced.

Table 2. Chemical families and temperature and pressure ranges of the pure compounds tested.

Substance	Formula	Family	Temperature [K]	Pressure [Mpa]	N
Acetone	C_3H_6O	Ketone	[178.50, 495.00]	[2.3e-6, 3.86]	23
Ammonia	H_3N	Light Gas	[195.50, 400.00]	[6.1e-3, 10.30]	22
Carbon Dioxide	CO_2	Light Gas	[216.59, 301.59]	[5.2e-1, 6.96]	35
Ethane	C_2H_6	Paraffin	[90.35, 300.35]	[1.1e-6, 4.39]	43
Ethylene	C_2H_4	Olefin	[103.99, 275.00]	[1.2e-4, 4.27]	19
Methane	CH_4	Paraffin	[90.69, 185.69]	[1.2e-2, 3.95]	20
Nitrogen	N_2	Element	[63.15, 125.00]	[1.2e-2, 3.21]	32
Oxygen	O_2	Element	[54.36, 154.36]	[1.5e-4, 5.00]	41

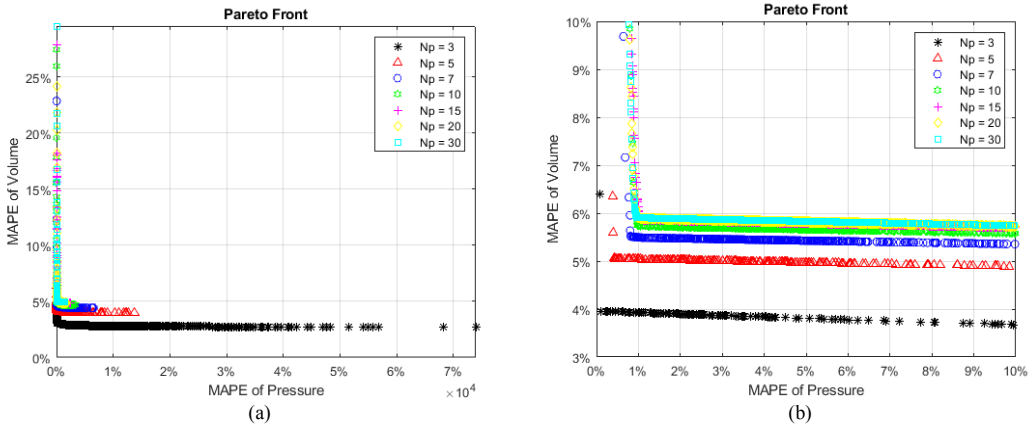


Figure 1. Optimization results for Acetone considering different number of experimental points: (a) Pareto fronts and (b) zoom of Pareto fronts.

The obtained values for the parameters C_1, C_2 and C_3 of GEOS3C equation of state through multiobjective optimization, for the three points mentioned above, are presented in Table 3.

Finally, optimal Pareto set for ethane is presented in Fig. 3. Once again, similar results were obtained for the other substances. As it can be seen in the projections' graphs, C_1 parameter of the GEOS3C equation of state seems to assume a constant value in relation to parameters C_2 and C_3. The two latter, on the other hand, seem to be linearly dependent on each other. It is important to highlight that in a mono-objective optimization approach it would not be possible to observe such characteristic, in view of the fact that only a single solution would be obtained.

Correlation Between the Parameters of the GEOS3C Equation of State

To analyse whether the hypothesis of correlation between the parameters of the GEOS3C equation of state is valid, part of the viable regions of the Pareto fronts were selected, taking into account a more proportional gain between the objective functions. In this analysis, C_1 parameter assumes a constant value, being the mean of the values obtained in the viable regions of the optimal Pareto sets, whereas C_2 and C_3 parameters are linearly correlated.

Linear relations provided by Matlab's Curve Fitting Tool are displayed in Table 4, as well as the Sum of Squares due to Error (SSE), which measures the total deviation between adjusted and predicted values, and the Multiple Correlation Coefficient (R-square), which is the square of the correlation between the adjusted and predicted values associated with each expression. It is important to highlight that both statistical parameters (SSE and R-square) present reasonable values for all linear relations, since a low SSE indicates a good fit of the model to the data and, the closer to unity is the R-square, the better the linear model is adjusted to the sample.

In Fig. 4, the linear relation displayed in Table 4 for oxygen is plotted against the obtained optimization results for parameters C_2 and C_3 in the viable regions, as well as the respective residuals. Similar results were obtained for the other substances. It is noted that in the considered regions there is a good agreement between the results of the multiobjective optimization and the

linear relation provided by Matlab, since the residuals oscillate around zero.

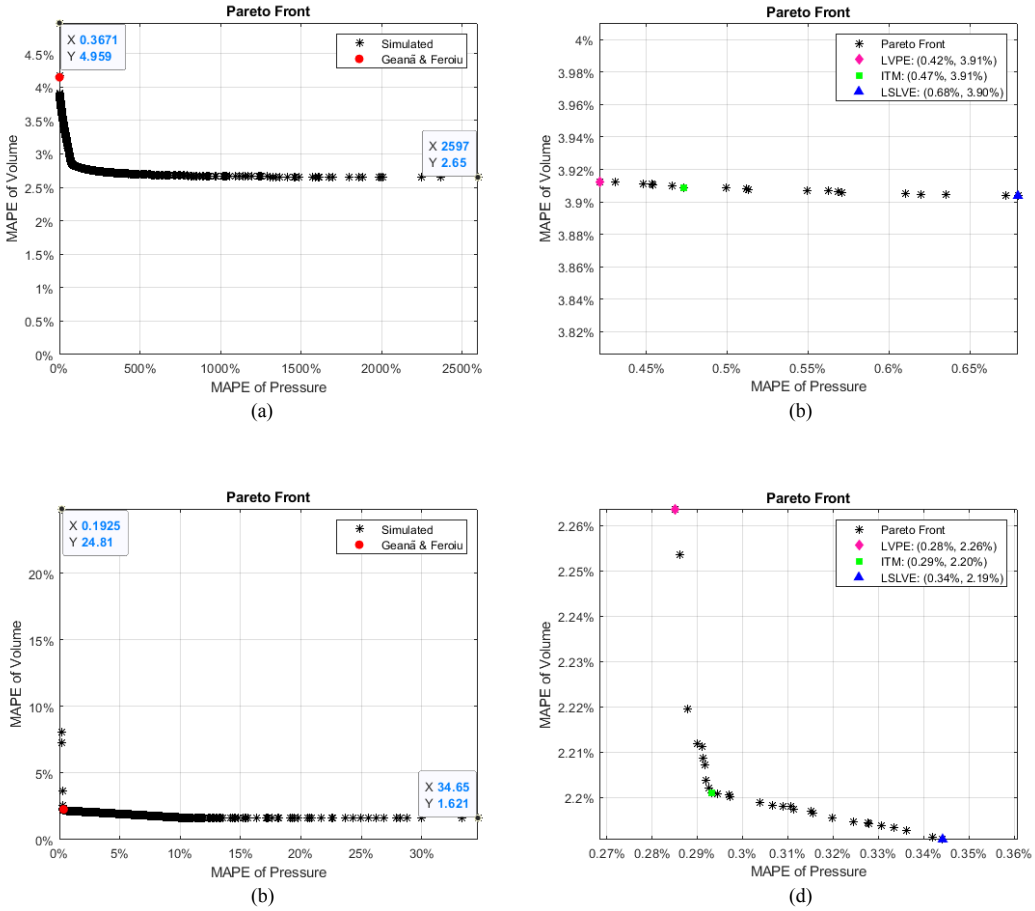


Figure 2. Pareto fronts (PF) obtained for two types of paraffins, with a zoom in the viable regions (VR): (a) PF - Ethane, (b) VR - Ethane, (c) PF - Methane and (d) VR - Methane.

Table 3. Optimal values obtained for the parameters of the GEOS3C equation of state for all tested substances.

Substance	C_1			C_2			C_3		
	LVPE(1)	LSLVE(2)	ITM(3)	LVPE	LSLVE	ITM	LVPE	LSLVE	ITM
Acetone	0.2090	0.1804	0.1800	10.106	0.9111	10.632	-0.9986	-0.6365	-10.491
Ammonia	0.1836	0.1787	0.1784	0.9595	0.9145	0.9736	-10.584	-0.8704	-10.826
Carbon Dioxide	0.2403	0.2564	0.2556	0.3284	0.1481	0.2807	17.839	29.297	19.311
Ethane	0.2186	0.2186	0.2186	0.3660	0.3446	0.3575	-0.1475	-0.0939	-0.1287
Ethylene	0.2076	0.2077	0.2075	0.3244	0.2691	0.3000	-0.0110	0.1591	0.0547
Methane	0.1037	0.1091	0.1090	0.2816	0.2416	0.2664	-0.0483	0.0852	-0.0141
Nitrogen	0.1402	0.1566	0.1565	0.2600	0.1599	0.2231	0.1426	0.4614	0.1986
Oxygen	0.1007	0.1600	0.1601	0.3493	0.1984	0.2390	-0.1433	0.0942	-0.0277

(1) Lowest vapor pressure error; (2) Lowest saturated liquid volume error; (3) Intermediate.

In Fig. 5 a comparison between the viable regions obtained through multiobjective optimization and the Pareto fronts obtained with the assumed correlations between C_1, C_2 and C_3 parameters of GEOS3C equation of state is presented for carbon dioxide and oxygen. Similar results were obtained for the other substances. As it can be seen, there is a good agreement between both data sets and, therefore, the consideration made here seems acceptable, ie, parameters C_1, C_2 and C_3 of GEOS3C equation of state are correlated in the selected interest ranges of Pareto fronts.

Thermodynamic Properties Calculation

Utilizing the values for the parameters C_1, C_2 and C_3 of GEOS3C equation of state obtained through multiobjective optimization, displayed in Table 3, as well as the ones available in Geanã and Feroiu (2000a)'s work, the following thermodynamic properties were calculated: saturation pressure (P_s), saturated liquid volume (V_l), saturated vapor volume (V_v), enthalpy of vaporization (ΔH^{vap}), entropy of vaporization (ΔS^{vap}), internal energy of vaporization (ΔU^{vap}), heat capacity at constant pressure of vaporization (ΔC_p^{vap}) and heat capacity at constant volume of vaporization (ΔC_v^{vap}). The vaporization properties were calculated using the residuals functions provided by Geanã and Feroiu (2000b) in the Appendix, for a given temperature and pressure, and the ideal gas contribution to the heat capacities at constant pressure and volume was calculated using the function recommended in Poling *et al.* (2001).

In order to make a quantitative comparison, the relative Average Absolute Deviations (AAD%) were calculated. For a given property *Y*, AAD% expression is

$$\mathrm{AAD\%} = \frac{100}{N}\sum_{i=1}^{N}\left|\frac{\left(Y_i^{eos} - Y_i^{exp}\right)}{Y_i^{exp}}\right| \qquad (25)$$

where Y_i^{exp} correspond to the experimental values, Y_i^{eos} to the values obtained using the equation of state and *N* to the number of experimental points.

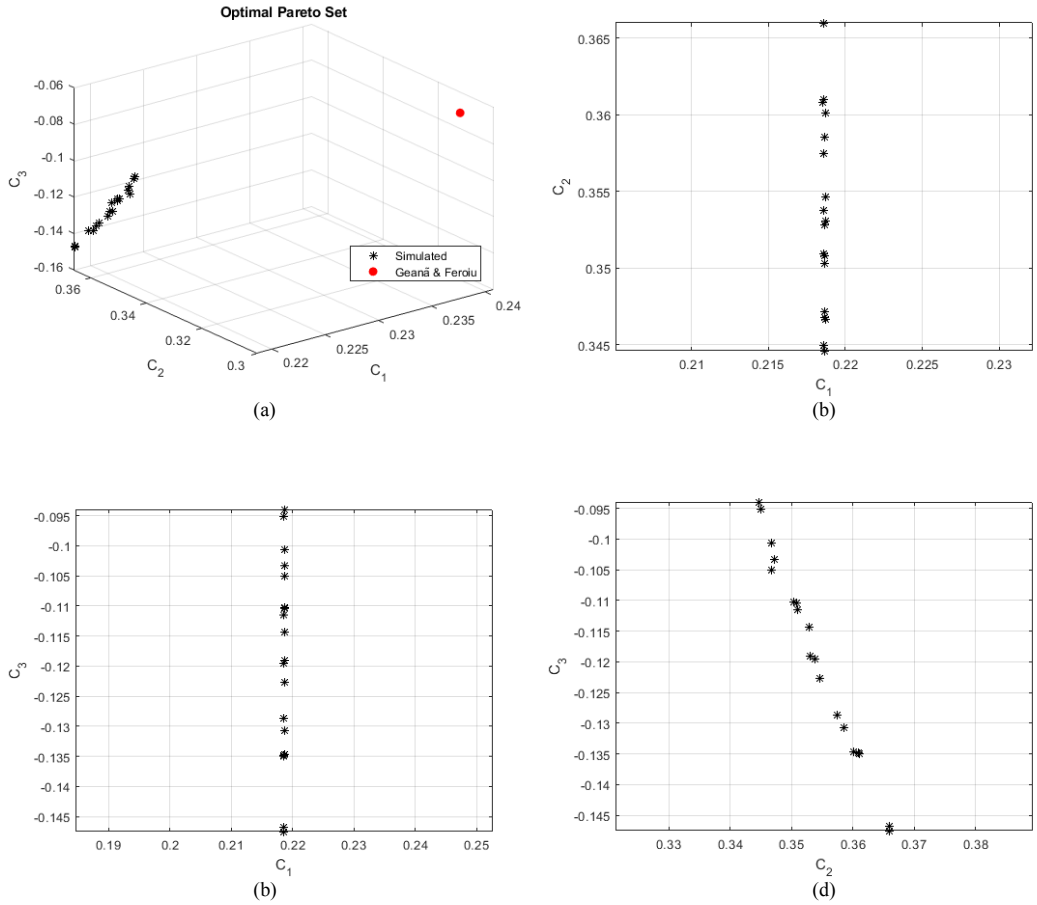
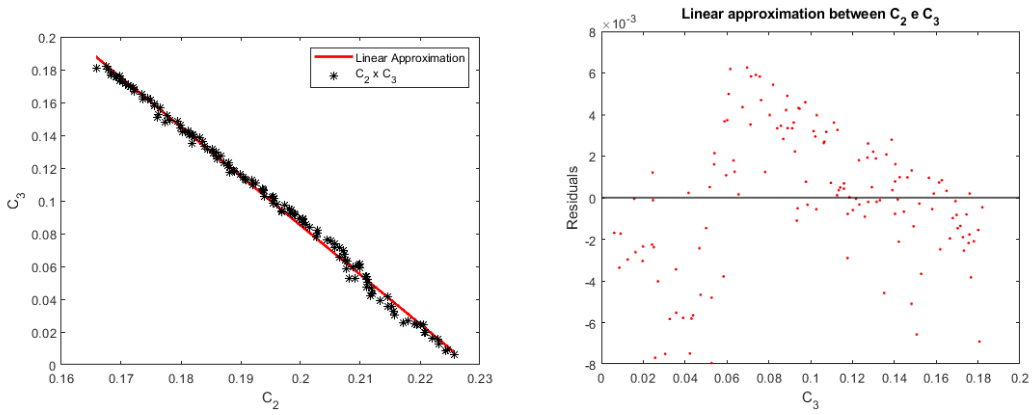


Figure 3. Optimization results for Ethane: (a) optimal Pareto set, (b) projection C_1 x C_2, (c) projection C_1 x C_3 and (d) projection C_2 x C_3.

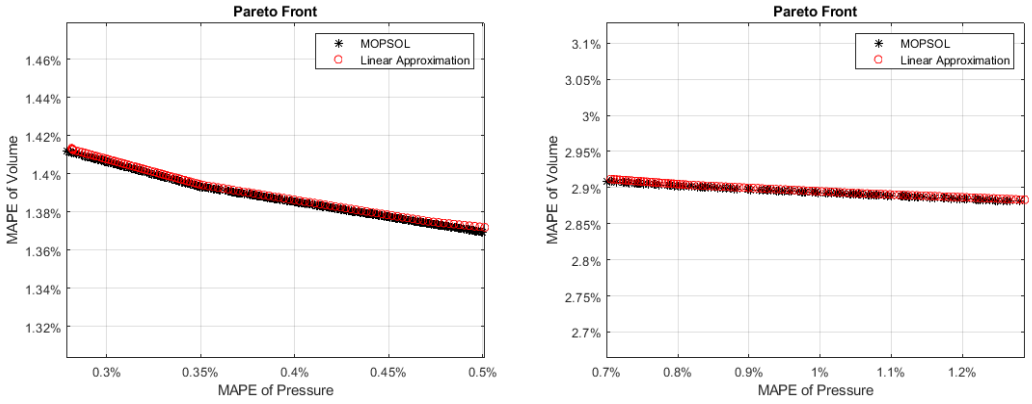
Table 4. Linear relations between the parameters of the GEOS3C equation of state provided by Matlab's Curve Fitting Tool for all tested pure compounds.

Substance	Linear Relation	SSE	R-square
Acetone	$C_3 = -2.54\ C_2 + 1.65$	1.79e-4	9.98e-1
Ammonia	$C_3 = -3.75\ C_2 + 2.56$	3.00e-3	9.99e-1
Carbon Dioxide	$C_3 = -7.23\ C_2 + 4.00$	4.10e-3	1.00
Ethane	$C_3 = -2.50\ C_2 + 0.76$	2.10e-3	9.80e-1
Ethylene	$C_3 = -3.07\ C_2 + 0.98$	1.70e-4	9.95e-1
Methane	$C_3 = -3.74\ C_2 + 0.99$	1.40e-3	9.99e-1
Nitrogen	$C_3 = -3.95\ C_2 + 1.09$	2.40e-3	9.99e-1
Oxygen	$C_3 = -3.00\ C_2 + 0.69$	1.40e-3	9.96e-1



(a) (b)

Figure 4. Correlation between C_2 and C_3 parameters of GEOS3C equation of state in the viable region of Pareto front for Oxygen: (a) linear approximation and (b) associated residuals.



(a) (b)

Figure 5. Comparison between the viable regions of MOPSOL and the Pareto fronts obtained with the linear approximations: (a) Carbon Dioxide and (b) Oxygen.

Experimental values for the properties were obtained in Green and Perry (2019) and Linstrom (2005) references. Temperature and pressure ranges, as well as the number of experimental points, used in thermodynamic properties calculation are displayed in Table 2.

In Tables 5-6, the relative average absolute deviations of the calculated thermodynamic properties for each tested substance are presented. For a matter of

space, only the results for the parameters of the GEOS3C equation of state obtained through multiobjective optimization that lead to the lowest deviations are shown, in the columns labeled "Opt". Subscripts p, v and i refer to the parameters associated to the lowest vapor pressure error, the lowest saturated liquid volume error and intermediate, respectively, presented in Table 3.

The following observations can be made: (1) There is a good improvement for some of the tested substances with respect to the properties directly used in the multiobjective optimization problem (P_s and V_l), as well as ΔH^{vap}, ΔS^{vap} and ΔU^{vap}. As an example, the AAD% associated with V_l prediction for oxygen had a reduction from 6.60% to 3.06%, the AAD% associated with P_s prediction for ethane had a reduction from 0.62% to 0.39%, and the AAD% associated with ΔH^{vap}, ΔS^{vap} and ΔU^{vap} predictions for acetone had a reduction from 2.68, 2.59 and 2.77% to 1.25, 1.42 and 1.28%, respectively; (2) For the saturated vapor volume V_v, both sets of parameters give equivalent results in most cases; (3) AAD% are relatively high for the heat capacities at constant pressure ($C_p^{l,v}$) and volume ($C_v^{l,v}$) in the liquid and vapor phases, respectively. This was already expected since it is known that classical cubic equations of state are not able to predict the correct divergent behavior of these properties near the critical region (Geanã and Feroiu, 2000b).

Finally, in Fig. 6, some of the calculated thermodynamic properties of ammonia as functions of the reduced temperature are presented. As it can be observed, there is a good agreement between experimental data and the ones obtained through the use of the GEOS3C equation of state, using both sets of parameters (Geanã & Feroiu and intermediate), for the properties directly used in the multiobjective optimization problem (Fig. 6 (a)-(b)). Similar results were obtained for V_v, ΔH^{vap}, ΔS^{vap} and ΔU^{vap} (not shown here). However, for the heat capacities at constant pressure and volume of vaporization (Fig. 6 (c)-(d)), that depend on the second derivative of GEOS3C temperature function, results are slightly divergent at some parts of the curves, which justifies the high AAD% obtained previously.

Table 5. AAD% of some thermodynamic properties for all tested substances as a function of different values for the GEOS3C equation parameters - Part I.

Substance	P_s		V_l		V_v		ΔH^{vap}		ΔS^{vap}	
	Opt.[(1)]	GF[(2)]	Opt.	GF	Opt.	GF	Opt.	GF	Opt.	GF
Acetone	3.79_p	2.40	6.14_v	6.92	1.49_p	1.48	1.25_v	2.68	1.42_v	2.59
Ammonia	0.51_i	0.57	4.22_v	4.33	2.28_p	2.27	2.17_p	2.31	2.19_p	2.30
Carbon Dioxide	0.27_i	0.30	1.40_v	1.90	3.82_v	3.73	5.05_i	5.08	5.06_i	5.08
Ethane	0.39_i	0.62	3.90_v	4.32	1.57_v	1.54	1.59_p	1.58	1.64_p	1.61
Ethylene	0.98_v	0.63	3.51_v	3.54	1.74_v	1.76	1.93_p	2.03	1.95_p	2.07
Methane	0.29_i	0.32	2.23_v	2.31	2.28_v	2.26	2.68_i	2.78	2.72_i	2.80
Nitrogen	0.35_p	0.46	2.24_v	2.55	2.47_v	2.45	3.20_i	3.00	3.24_i	3.05
Oxygen	0.56_p	0.92	3.06_v	6.60	1.95_v	1.84	2.85_i	2.75	2.91_i	2.78

(1) Optimization results. Subscripts *p*, *v* and *i* refer to the parameters associated to LVPE, LSLVE and ITM, respectively;
(2) Geanã & Feroiu (2000).

Table 6. AAD% of some thermodynamic properties for all tested substances as a function of different values for the GEOS3C equation parameters - Part II.

Substance	ΔU^{vap}		C_p^l		C_p^v		C_v^l		C_v^v	
	Opt.[(1)]	GF[(2)]	Opt.	GF	Opt.	GF	Opt.	GF	Opt.	GF
Acetone	1.28_v	2.77	52.06_v	57.65	94.90_p	94.81	56.59_v	64.72	87.90_i	87.86
Ammonia	2.11_p	2.25	28.57_v	30.15	87.26_p	87.22	30.11_v	32.59	73.49_i	73.54
Carbon Dioxide	5.06_i	5.15	13.67_v	14.25	73.19_v	73.12	28.29_p	36.29	70.48_v	70.83
Ethane	1.55_p	1.55	45.38_v	45.62	89.76_p	89.73	41.79_v	42.48	74.52_p	74.60
Ethylene	1.91_p	2.01	36.99_v	38.29	87.82_p	87.84	29.09_v	30.90	70.14_p	70.13
Methane	2.67_i	2.79	39.54_v	39.89	83.65_i	83.65	37.61_v	38.48	68.62_p	68.76
Nitrogen	3.18_i	2.97	30.24_v	33.69	80.47_i	80.37	24.46_v	27.08	62.75_p	62.98
Oxygen	2.81_i	2.74	37.95_v	39.48	84.28_i	84.15	28.71_v	32.85	62.99_p	63.92

(1) Optimization results. Subscripts *p*, *v* and *i* refer to the parameters associated to LVPE, LSLVE and ITM, respectively;
(2) Geanã & Feroiu (2000).

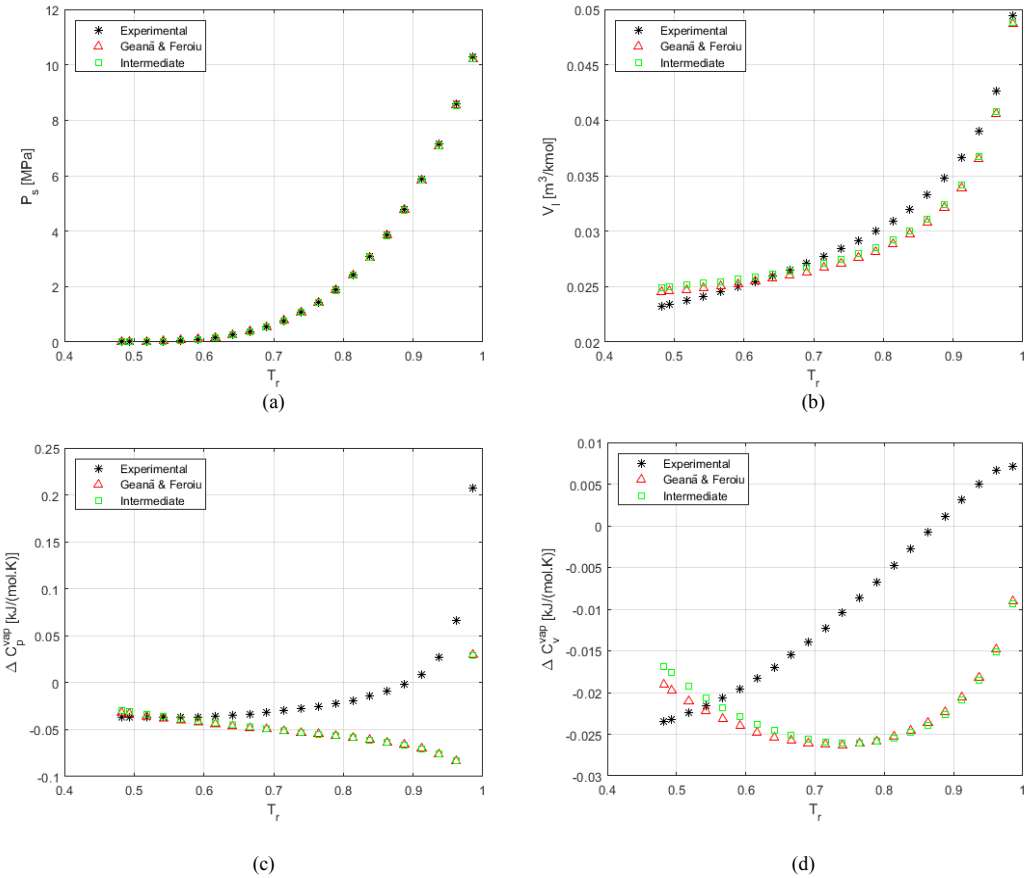


Figure 6. Thermodynamic properties as functions of the reduced temperature for ammonia, using the GEOS3C equation parameters of Geanã and Feroiu and the intermediate ones obtained through multiobjective optimization: (a) P_s, (b) V_l, (c) ΔC_p^{vap} and (d) ΔC_v^{vap}.

CONCLUSIONS

In this work, a new methodology to estimate temperature function's parameters (C_1, C_2 and C_3) of GEOS3C equation of state is proposed, using multiobjective optimization. A modified version of MOPSO algorithm was employed in this process, taking into account the parameters that lead to the lowest errors of vapor pressures and saturated liquid volumes predictions.

Through the obtained Pareto fronts results, it was possible to notice a linear correlation between C_2 and C_3 parameters in the viable regions. Besides, C_1 showed to assume a constant value. This kind of analysis was only possible due to the fact that in a multiobjective optimization problem a set of solutions is obtained, instead of a single one.

Substances from different chemical families were used to evaluate the methodology proposed in this work and comparisons with experimental data available in the literature were made. The results showed that the new sets of values obtained for the parameters of the GEOS3C equation of state through multiobjective optimization provide better or equivalent predictions for the calculated thermodynamic properties in almost all cases tested, having the main advantage of being possible to choose those that privilege a given property of interest.

In a future work, authors intend to expand the results for more substances and from different chemical families in order to analyse if the observations made here can be applied to a significant group of pure compounds.

ACKNOWLEDGEMENTS

This study was financed in part by the Coordenação de Aperfeiçoamento de Pessoal de Nível Superior - Brasil (CAPES) - Finance Code 001.

RESPONSIBILITY NOTICE

The authors are solely responsible for the printed material included in this paper.

REFERENCES

Abdollahi-Demneh, F., Moosavian, M., Montazer-Rahmati, M., Omidkhah, M. and Bahmaniar, H., 2010. "Comparison of the prediction power of 23 generalized equations of state: Part I. Saturated thermodynamic properties of 102 pure substances". Fluid phase equilibria, Vol. 288, No. 1-2, pp. 67–82.

Coello, C.C. and Lechuga, M.S., 2002. "Mopso: A proposal for multiple objective particle swarm optimization". In Proceedings of the 2002 Congress on Evolutionary Computation. CEC'02 (Cat. No. 02TH8600). IEEE, Vol. 2, pp. 1051–1056.

Coello, C.A.C., Pulido, G.T. and Lechuga, M.S., 2004. "Handling multiple objectives with particle swarm optimization". IEEE Transactions on evolutionary computation, Vol. 8, No. 3, pp. 256–279.

Eberhart, R. and Kennedy, J., 1995. "A new optimizer using particle swarm theory". In MHS'95. Proceedings of the Sixth International Symposium on Micro Machine and Human Science. Ieee, pp. 39–43.

Geanã, D., 1986. "New equation of state for fluids. 1. Application to pvt calculi for pure fluids". Revista de Chimie, Vol. 37, No. 5, pp. 303–309.

Geanã, D. and Feroiu, V., 2000a. "A new parametrization of the general cubic equation of state and PVT properties for pure fluids".

Geanã, D. and Feroiu, V., 2000b. "Thermodynamic properties of pure fluids using the geos3c equation of state". Fluid phase equilibria, Vol. 174, No. 1-2, pp. 51–68.

Green, D.W. and Perry, R.H., 2019. Perry's Chemical Engineers' Handbook/edición Don W. Green y Robert H. Perry. C 660.28 P47 2008.

Soares, A.M., Mota, B.T., Pena, L.P. and Pires, A.P., 2020. "Adaptação do algoritmo PSO para problemas multiobjetivo, Iterações com liderança global fixa". Proceeding Series of the Brazilian Society of Computational and Applied Mathematics, Vol. 7, No. 1.

Laumanns, M., Thiele, L., Deb, K. and Zitzler, E., 2002. "Combining convergence and diversity in evolutionary multiobjective optimization". Evolutionary computation, Vol. 10, No. 3, pp. 263–282.

Linstrom, P.J., 2005. "Nist chemistry webbook". http://webbook. nist. gov.

Menegazzo, T.A., Junior, A.M.S., Mota, B.T., Henderson, N. and Pires, A.P., 2019. "Application of an equation of state incorporating association to alcohols up to decanol". Fluid Phase Equilibria, Vol. 482, pp. 24–37.

Monroy-Loperena, R., 2012. "A note on the analytical solution of cubic equations of state in process simulation". Industrial & engineering chemistry research, Vol. 51, No. 19, pp. 6972–6976.

Mota, B.T.S., 2019. Estimação de parâmetros de modelos termodinâmicos via otimização multiobjetivo. Ph.D. thesis, Universidade do Estado do Rio de Janeiro, Nova Friburgo.

Patel, N.C. and Teja, A.S., 1982. "A new cubic equation of state for fluids and fluid mixtures". Chemical Engineering Science, Vol. 37, No. 3, pp. 463–473.

Poling, B.E., Prausnitz, J.M., O'connell, J.P. et al., 2001. The properties of gases and liquids, Vol. 5. Mcgraw-hill New York.

Rackett, H.G., 1970. "Equation of state for saturated liquids". Journal of Chemical and Engineering Data, Vol. 15, No. 4, pp. 514–517.

Terron, L.R., 2009. Termodinâmica química aplicada. Manole.

Wagner, W., 1977. "A new correlation method for thermodynamic data applied to the vapor pressure curve of argon, nitrogen and water". IUPAC Thermodynamic Tables Project Centre, Department of Chemical Engineering and Chemical Technology, Imperial College of Science and Technology.